International Journal of Sciences & Applied Research

www.ijsar.in

Capping agents influence on structure, optical behaviour and Glucose oxidase mobilization on ZnS QDs: in Glucose sensors viewpoint

Sarita Narkhede[1] and Smita A. Acharya[2]*

[1]Shrimati Radhikatai Pandav, Polytechnique College, Nagpur-440015, M.S. India.
[2]Department of Physics, RTM Nagpur University, Nagpur-440033, M.S. India.

Correspondence Address: *Smita A. Acharya, Department of Physics, RTM Nagpur University, Nagpur-440033, M.S. India.

Abstract

In the present attempt, water soluble ZnS QDs were successfully synthesised using different capping agents polyvinalpyrolidone (PVP), mercapto propanic acid (MPA), 2-mercapto ethanol (ME), hydrazine hydrate (HH) and thioglycerol (TG) by co-precipitation route. X-ray diffraction (XRD) study confirms zinc blende structure of all ZnS samples. Transmission Emission microscopy (TEM) images exhibit fine scale spherical particles having size varying in between 7 to 15 nm thus ensure QDs formation. UV-VIS absorption spectra show blue shift in absorption peaks in almost all samples; however for ME-ZnS the shift is largest and PVP-ZnS it is smallest. Capping agents induced blue shift in absorption peak attribute to variation in size of QDs. Ligands existence with ZnS QDs are also confirmed by Fourier Transform Infrared spectroscopy (FTIR). A typical room temperature photoluminescence (PL) spectrum of ZnS QDs shows that the spectrum is dominated by characteristics deep level emission peak in between 500 and 550 nm, correlated with transition from conduction band to sulphur vacancies defect structure, which acts as doubly ionized donor centres. The PL spectra of capped-ZnS QDs bioconjugated by glucose oxidase (GOx) enzymes are effectively quenched with glucose content. The kinetics of the enzymatic-catalyzed reaction are estimated by Michaelis-Menton kinetic parameters (K_m and Vmax). The values of K_m and V_{max} exhibit that PVP as capping agents are more supportive for GOx mobilization on ZnS and respective enzymatic activity.

Keywords: ZnS QDs, capping agents, GOx mobilization, Glucose sensors

Introduction

II–VI or III–V groups semiconductor quantum dots (QDs) are extensively focused due to their unique physical properties in general and optical properties in particular [1-6]. QDs possess very high photo stability, tuneable fluorescence under single wavelength excitation and longer life time as compared to conventional fluorophores. The origin of these properties arises from the confinement of the states of charge carriers due to size effect. Recent developments show a promising future of semiconductor QDs for biological applications [7- 10]. Biological processes originated from biological entities such as antibodies, enzymes, nucleic acids, peptides etc are bioconjugated on QDs. Semiconductor QDs

can be extensively utilized for these purposes as substrate [11-16]. However bare uncoated QDs cannot be used directly for biological applications [17]. The typical QDs-biomolecules bioconjugate is comprised of three main components: (1) QDs as core (ii) an interfacial organic coating on core and (iii) conjugate biomolecules as a shell. The incorporation of semiconductor QDs with biomolecules has been motivated by the idea of bringing the unique, intrinsic properties of QDs into biological environments and experiments [18]. At the surrounding of the QDs, the organic coating functions to disperse the QDs in an aqueous solution and, ideally, in more complex physiological environments. Many coatings are multifunctional in nature, displaying, at minimum, some chemical functionality that tightly associates with the inorganic interface of the QDs and another that interacts favourably with water to provide stable colloidal dispersion. The interface organic coating may be neutral, anionic, cationic or compact functional groups or oligomer [19-21]. These provide complimentary reactive site for bioconjugation, thus affect on: (1) the number of biomolecules conjugated on QDs, (ii) The orientations of biomolecules on QDs, (iii) the distance separating the biomolecules from QDs, (iv) the affinity or stability of biomolecules on the QDs, consequently decides the rate of catalytic activity. So there is need to choose the coating agent of QDs carefully as it directly affect on enzymatic activity. The development of coatings that maintains QDs dispersion over a wide range of biological relevant conditions continues to be a very active area of research. So in the present attempt, role of different interface organic coating agent on bioconjugation of glucose oxidase (GOx) on ZnS QDs and respective enzymatic activities for glucose sensing are systematically examined.

Experimental procedure

Zinc chloride ($ZnCl_2$), sodium sulphide (Na_2S . $9H_2O$) and different reducing agents like polyvinalpyrolidone (PVP), mercapto-propanic acid (MPA), 2-mercapto ethanol (ME), hydrazine hydrate (HH) and thioglycerol (TG) were procured from Sigma Aldrich. All the reagents were of analytical grade and used without further purification. Ultrapure water was used for synthesis of ZnS. Co-precipitation approach was used for synthesize of ZnS QDs by using different capping agents.1.3628 g zinc chloride ($ZnCl_2$) was added in 100 ml ultrapure water with vigorous stirring at 70^0C. After complete dissolution of $ZnCl_2$ in water, 0.08 g PVP was inserted and stirred it for three hours. Separately prepared 0.7804 gNa_2S + 100 ml ultrapure water solution was added drop wise with vigorous stirring until it appears completely milky white. This sample were kept overnight for stabilization. The samples were washed several times by centrifugation using deionised water. The procedure was repeated for different capping agents ME, MPA, HH and TG.

Result and Discussion

Fig 1 shows XRD patterns of as-synthesized ZnS quantum dots by using different capping agent. The broadened diffraction peaks compared to those of the bulk ZnS crystals, signifying the fine size of these crystallites. The diffraction peaks are detected around 28.79°, 47.87°, and 56.30°. These peaks are identified due to (111), (220), and (311) planes of cubic or zinc blende structures of ZnS (JCPDS no. 5-566). More careful observation of XRD data depict that the peak at (111) is found to be shifted at lower angle side for ME and PVP capped ZnS as compared to others capping agents. The straining effect due to variation of quantum size may attribute to this effect. The broad nature of XRD peak can be used to estimate the size of ZnS QDs by Debye Scherrer formula

$$D = \frac{0.9\lambda}{\beta cos\theta} \quad (1).$$

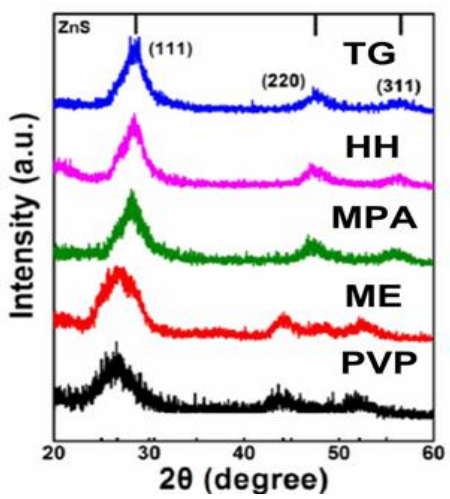

Fig. 1: XRD pattern of as-synthesized ZnS quantum dots synthesized by using different ligands.

All variables have their usual meaning. The estimated sizes of ZnS QDs, by using different capping agents are tabulated in table 1. For ME-ZnS size of QDs are obtained to be 7nm, while PVP-ZnS are 9nm. For other capping agents sizes of ZnS QDs are varying in between 11 - 15 nm.

Table 1: Particle size estimation by XRD, TEM and UV-VIS spectra.

Sample	QDs size estimation in (nm)		
	XRD	TEM	UV
PVP-ZnS	9	6	5
ME-ZnS	7	8	7
MPA-ZnS	11	10	9
HH-ZnS	14	13	12
TG-ZnS	15	16	13

Transmission electron microscopy (TEM) images (see Fig 2) reveal that the QDs particles are spherical in shape and almost uniform in size. The diameter of QDs is dependent dominantly varying with capping agent. The mean particle size estimated from the histograms was 6 nm, and 8 nm,10 nm, 13 nm and 16 nm correspond to ME, PVP, MPA, HH, and TG-capping agents, respectively. It indicates that the crystallites size are highly manipulating by capping agents.

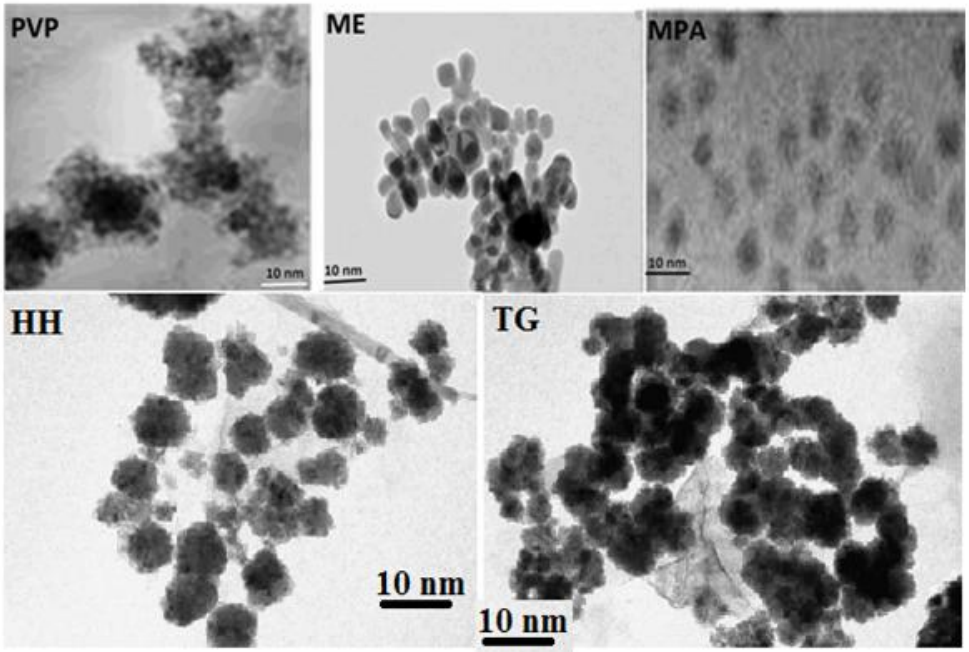

Fig. 2: TEM images of capped-ZnS QDs.

Optical Absorption

The UV-absorption spectra capped-ZnS QDs synthesized with different capping agents are shown in Fig 3. The absorption peaks shifts to lower wavelength from 325 (bulk) through 315, 310, 302, 297 to 285 nm. The variation in wavelength of absorption peak for different capping agents can be attributed to size effect of QDs. The optical absorption spectra show the blue shift due to decrease in particle size. Higher blue shift is observed for ME-ZnS as compared to other capping agents indicates that the size and optical properties of ZnS QDs are tuneable by capping agents. The solid-state theory based on the delocalized electron and hole within the confined volume can explain the blue shift of absorption edge compared to bulk ZnS optical absorption spectra [21] The energy gaps were calculated using the Brus equation:

$$\Delta E = \frac{\hbar}{8r^2}\left[\frac{1}{m_e^*}+\frac{1}{m_h^*}\right]-\frac{1.8e^2}{4\pi\varepsilon_o\varepsilon_r} \quad (2)$$

where ΔE is the blue shift of the band gap, $m_e^* = 0.25\ m_e$, $m_h^* = 0.60\ m_e$, E_g is the bulk band gap in (ZnS = 3.7 eV), r- is the particle radius, ε_r is the dielectric constant and ε_o is the permittivity of free space. The first term indicates the confinement effect and the second term is the coulomb term. This second term is small due to the strong confinement and can be neglected. Different capping agents give different dimensions i.e. radius (r) to estimate band gaps using Eq. (2) as given in the Table 1. It is seen from the Table 1 that the sizes obtained via XRD, TEM and UV-VIS are fairly agreed.

Fourier transforms infrared spectroscopy (FTIR)

Existence of different capping agents on surface of QDs can be realized by FTIR spectra. The bonding between the capping agents molecules on SC-QDs are confirmed by FTIR in the range 4000 - 400 cm^{-1}. The FTIR spectra of 2ME, MPA, PVP-capped ZnS QDs are shown in Fig. 4. The FTIR spectrum of capped ZnS QDs exhibits broad transmission band centred at around 3480 cm^{-1} in almost all samples are attributed to O-H stretching mode of H_2O absorbed on the surface of the QDs. The peak between 1150 to 1650 corresponds to C-N and C=O stretching motion of monomer polymer of PVP, MPA and 2ME, respectively. The transmission mode around 1060 cm^{-1} are attributed to C=N stretching. In MPA capped ZnS, mode near 666 cm^{-1} is due to S-C vibration; However in 2ME-capped ZnS, vibration mode near 666 cm^{-1} are attributed to C-H out of plane bending.

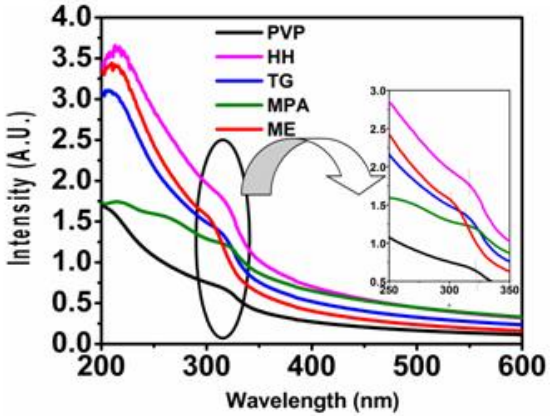

Fig. 3: UV-VIS of capped-ZnS QDs.

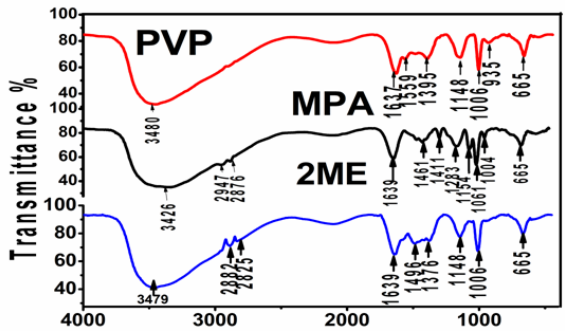

Fig. 4: FTIR spectra of ZnS QDs with PVP, MPA, 2ME as a stabilizing agent.

Table 1: Different FTIR transmission mode of capped ZnS QDs.

Sample	Wave numbers (cm^{-1})	Description of IR peaks
ZnS PVP	2833 1644, 1435, 1052, 1002 1415	C=O stretching C=N stretching CH_2 bending
ZnS MPA	3456 1642, 1632 1401. 1141 1308, 1060, 1009 666, 602, 596, 557	OH stretching of –COOH gp. and stretching of alkyl gp. Stretching of carbonyl gp. -C-H bending C-O stretching S-C vibration
ZnS 2ME	3333 1459, 1414 1286, 1059, 1005 666	OH stretching C-H bending of methylene C-O stretching C-H out of plane bending

The functional groups are present on the surface of prepared samples are easily attached with biomolecules. Generally OH (hydroxyl), COOH (carboxylic acid) and amine functionalities are present on the biomolecule surfaces (5). We can infer the presence of the organic layer coating on the QDs. Such types of functional groups on the surface of the QDs make them compatible with attached biomolecule. Another important point is that, we have preferred for aqueous medium to prepared QDs, as the result there is always hydrophobic surfaces of QDs which are directly conjugated to bio molecules and the hydrophobic surfaces have a need to other additional surface processing steps before conjugation. The linking mechanism is explained with the FTIR analysis and is tabulated in table 1.

Photoluminescence spectra

A typical room temperature photoluminescence (PL) spectrum of capped-ZnS QDs are shown in Fig 5. The spectrum is dominated by characteristics deep level emission peak about 500 to 550 nm respectively. The deep level emission is often attributed to stacking faults and non-stoichiometric defects such as intrinsic point defects (vacancies and interstitials). Vacancies and interstitials having different charged states (V_S, V^{+}_{S}, V^{2+}_{S}, V_{Zn}, V^{-}_{Zn}, Zn_i, Zn^{+}_{i}, Zn^{2+}_{i},S, S_i, S^{2}_{i}) introduced different localized energy levels within the band gap and also combine into donor-acceptor pairs. S vacancies and Zn interstitials introduce energy levels close to the edge of the conduction band hence acts as donor states. However S interstitials and Zn vacancies introduced energy levels closer to the edge of the valence band hence acts as acceptor levels. The observed PL emission bands for capped-ZnS after excitation by 340 nm correspond to transition from conduction band to S vacancies. The observed PL emission band in visible range makes us to use ZnS QDs for biological application.

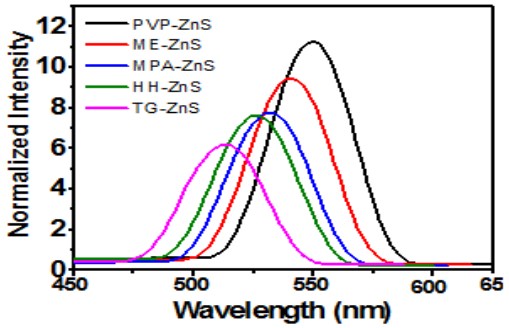

Fig. 5: PL spectra of capped-ZnS.

Enzymatic activity of GOx on capped-ZnS QDs: as glucose sensors

Influence of capping agents used for ZnS on bioconjugation of GOx and respective enzymatic activity for glucose sensing view point are studied systematically. For bioconjugation of GOx-capped ZnS, glucose oxidase was dissolved in phosphate buffer saline solution (PBS, 10 mm, P_H 7.4) to obtain a solution (1.00 mg mL^{-1}) that was stored at 4^0C. The conjugation proceeds by N-hydroxysuccinimide (NHS) and 1-ethyl-3-(3-dimethylaminopropyl) carbodiamide (EDC) forming active esters to conjugate the capping agents containing different organic group of ZnS QDs to primary amine groups of GO_X. EDC (0.50 mg) and NHS (0.25 mg) were added to ZnS QDs stock solution (1.00 ml) to activate the QDs in PBS and it was incubated at 30 min at room temperature with continuous gentle mixing. Next, the activated quantum dots (25 µl) and GOx solution were incubated at room temperature for another 2 h with continuous gentle mixing and then stored at 4^0 C.

H_2O_2 has been reported to be an effective quencher for CdSe@ZnS or CdTe QDs, which are the product enzymatic processes of GOx. The coupling of QDs with these enzymes provides promising biosensing strategy without extra quenching units for QDs. However, PL spectra of GOx – MPA and PVP capped-ZnS QDs bioconjugate (see Fig 6a and b, respectively), which are also found effectively quench with glucose content. The PL emission of ZnS QDs are correlated with transition from conduction band to sulphur vacancies defect structure, which acts as doubly ionized donor centres. It can be speculated as high surface to volume ratio in QDs, surface S^{2-} ions on the surface were oxidised to S which existed as defect in the product. The intense emission peak at this region may be due these defects.

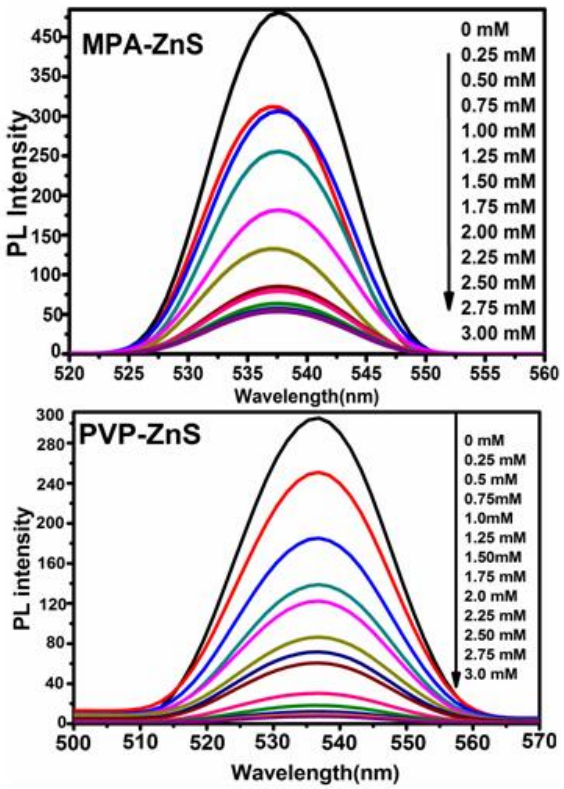

Fig. 6: Effect of Glucose content on the PL spectra of GOx + MPA-ZnS and PVP-ZnS.

The enzymatic activity can be estimated by using method proposed in earlier work by [22-23]. It clearly predicts that H_2O_2 production increases with increasing glucose content. The H_2O_2 is the quenching unit in the hybrid system. The extent of PL spectrum intensity quenching can be used to quantify the enzymatic activity (Fig 7). According to the theory of kinetics of enzymatic-catalyzed reaction, Michaelis-Menton kinetic parameters (K_m and V max), can be determined by the analysis of enzyme-substrate reactions. The K_m parameter is used to estimate the affinity of the enzyme for the substrate in enzymatic reaction. V_{max} provides the maximum rate of enzymatic reaction when the enzyme is saturated by the substrate. These parameters have been estimated using the Lineweaver-Burke plot, that is, the inverse of absorption versus the inverse of glucose concentration.

The inverse of the intercepts at the x-axis and y-axis gives the value of K_m and V_{max} respectively. The smaller value of K_m indicates the increased affinity of enzyme for substrate. The values of K_m in the present enzymatic assay are found to be 4 mM/L, 2.39 mM/L, 2.66 mM/L, 2.83 mM/L and 2.83 mM/L for the PVP, HH, TG, ME and MPA as-capping agents for ZnS respectively. While, the respective values of V_{max} are obtained to be 0.5, 0.43, 0.32, 0.21 and 0.12. It clearly indicates that enzyme affinity is affected by capping agents and is more for PVP.

Conclusion

ZnS QDs were successfully synthesised by soft chemical route by using different capping agents. XRD confirms zinc blende structure of all ZnS samples. TEM images exhibit fine scale spherical particles having size varying in between 7 to 15 nm thus ensure QDs formation. UV-VIS absorption spectra shows blue shift in absorption peaks of almost all samples; however for ME-ZnS the shift is largest and PVP-ZnS it is smallest. Capping agents modified blue shift attribute to variation in size of QDs. FTIR confirms existence of ligands on surface of ZnS QDs. A typical room temperature photoluminescence (PL) spectrum of ZnS shows that the spectrum is dominated by characteristics deep level emission peak in between 500 and 550 nm, correlated with transition from conduction band to sulphur vacancies defect structure, which acts as doubly ionized donor centres. The PL spectra of ZnS with different capping agents are effectively quenched with glucose content. The observed PL quenching of ZnS QDs + GOx conjugate by glucose content are due to trapping of electrons at the conduction band of QDs by H_2O_2 which is biproduct of enzymatic reaction of GOx and Glucose, hence radiative recombination rate of electrons and holes is slowed down, which decides the PL emission intensity. The kinetics of the enzymatic-catalyzed reactionare estimated by Michaelis-Menton kinetic parameters (K_m and Vmax). The values of K_m and V_{max} exhibits that PVP as capping agents are more supportive for GOx mobilization on ZnS QDs.

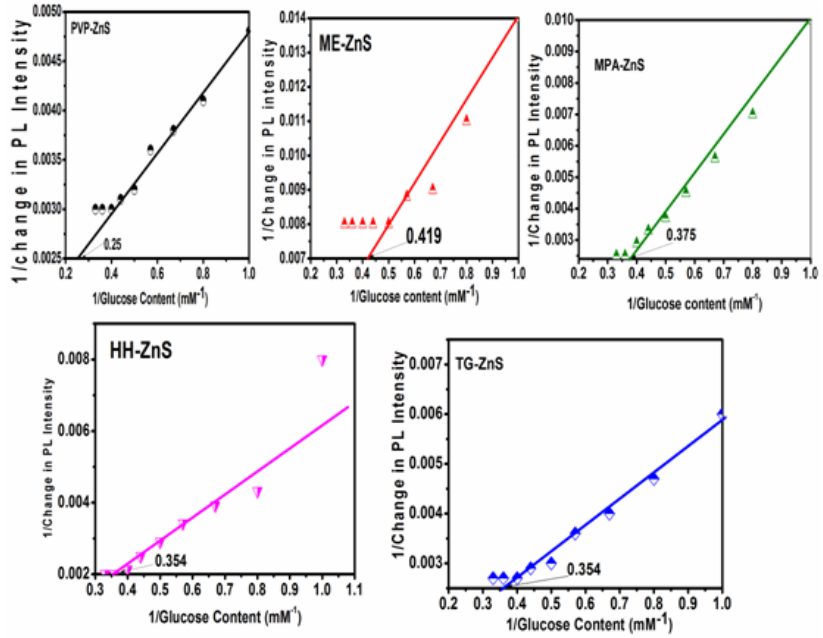

Fig. 7: Lineweaver-Burke plots of capped ZnS QDs.

References

[1] P. Zrazhevskiy, L.D. True, X. Gao Nat Protoc 8(10), 1852 (2013).

[2] P. Zrazhevskiy, M. Sena, X. Gao Chem Soc Rev. 39(11), 4326 (2010).

[3] W.C Chan, D.J. Maxwell, X. Gao, R.E Bailey, M. Han, S. Nie. Curr Opin Biotechnol, 13(1),40 (2002)

[4] Acaru Aurel Tab, Mus Viorica¸ T. Nicolae¸ S. Bogdan ¸ Tefan Vasilec, Vasile-Adrian Surduc, Applied Surface Science 359, 766 (2015).

[5] A. M. Alkilany, E.C. Dreaden, M.A. El Sayed, X. Huang, C.J. Murphy Chem. Soc.Rev. 41 (7) 2740 (2012).

[6] A. S. Karakoti, R. Shukla, R. Shanker, S. Singh, Advances in Colloid and Interface Science, 215, 28 (2015).

[7] Ru Xu, J. Yandong, X. Lei, T. Zhang, L. Xu, S. Zhang , D. Liu, H. Song, Biosensors and Bioelectronics 74, 411 (2015).

[8] R. Wahab, F. Khan, Lutfullah, R.B. Singh, A. Khan, Physica E 62, 111 (2014).

[9] Dudu Wua, Zhi Chen, Enzyme and Microbial Technology 51, 47(2012).

[10] Lei Tan,Cong Huang, Rongfei Peng, Youwen Tang,Weiming Li, Biosensors and Bioelectronics 61,506 (2014).

[11] I. Willner, B. Willner, Nano Letters 10, 3805 (2010).

[12] B.Y.S. Kim, J.T. Rutka, W.C.W. Chan, N. Engl. J. Med. 363, 2434 (2010).

[13] K.E. Sapsford, K.M. Tyner, B.J. Dair, J.R. Deschamps, I.L. Medintz, Anal. Chem. 83, 4453 (2011).

[14]] J.H. Gao, H.W. Gu, B. Xu, Acc. Chem. Res. 42 , 1097 (2009).

[15] J.H. Gao, B. Xu, Nano Today 4 37 (2009).

[16] W.R. Yang, P. Thordarson, J.J. Gooding, S.P. Ringer, F. Braet, Nanotech 18 (2007) 412001.

[17] B.Y.S. Kim, J.T. Rutka, W.C.W. Chan, N. Engl. J. Med. 363, 2434 (2010).

[18] L.O Cinteza. J Nanophotonics 4(1), 1 (2010).

[19] E. Oh, F. Fatemi, M. Currie, J.B. Delehanty, T. Pons, A. Fragola, S. Lévêque-Fort, R. Goswami, K. Susumu, A. Huston, I.L. Medintz, Part. Part. Syst. Charact. 30 453 (2013).

[20] W.R. Algar, K. Susumu, J.B. Delehanty, I.L. Medintz, Anal. Chem. 83 (2011) 8826—8837.

[21] K. Susumu, E. Oh, J.B. Delehanty, J.B. Blanco-Canosa, B.J. Johnson, V. Jain, W.J. Hervey, W.R. Algar, K. Boeneman, P.E. Dawson, I.L. Medintz, J. Am. Chem. Soc. 133, 9480 (2011).

[22] L. F. Shi, V. De Paoli, N. Rosenzweig, Z. Rosenzweig, J. Am. Chem. Soc., 128, 10378 (2006).

[23] P. Wu, Y. He, H. F. Wang, and X. P. Yan, Anal. Chem., 82, 1427 (2010).